

# Synthesis, characterization and photoelectrochemical properties of poly(3,4-dioctyloxythiophene)–CdS hybrid electrodes

Monika Refczynska, Józef Mieczkowski, Magdalena Skompska\*

*Department of Chemistry, Warsaw University, ul. Pasteura 1, 02-093 Warsaw, Poland*

Received 10 August 2007; received in revised form 2 November 2007; accepted 2 November 2007

Available online 13 November 2007

## Abstract

CdS–poly(3,4-dioctyloxythiophene) (CdS–PDOT) hybrid electrode has been prepared by electrosynthesis of PDOT on Au substrate followed by electrodeposition of Cd and its chemical transformation into CdS. The polymer and semiconductor obtained by this method form hemispherical structures dispersed on the substrate. The synthesized composites were characterized by UV–vis absorption spectra and energy dispersive X-ray spectra (EDS). The AFM images of the electrodes covered with different amounts of each component were correlated with photoactivity of the hybrid electrodes. Photoresponses of Au/PDOT–CdS electrodes under illumination in aqueous solution of Na<sub>2</sub>S were also compared with those of CdS without polymer. Enhancement of the photocurrent achieved for some polymer-to-semiconductor ratio is discussed in terms of the hybrid electrode morphology and hole-mediating properties of PDOT. The power conversion efficiency of the device based on CdS–PDOT hybrid electrode was determined from photocurrent–potential behavior of two electrode system, Au/CdS–PDOT/0.1 M Na<sub>2</sub>S/Pt with a variable resistance in series in the external circuit.

© 2007 Elsevier Ltd. All rights reserved.

**Keywords:** CdS; Poly(3,4-dioctyloxythiophene); Polymer–semiconductor hybrid electrode; AFM; Photovoltaic properties

## 1. Introduction

Conducting polymer–semiconductor hybrids represent a novel class of materials for low-cost photovoltaic devices. Combining of p-type conducting polymers and n-type semiconductors is advantageous for separation of the charges generated under illumination due to a high electron affinity of inorganic semiconductor and relatively low ionization potential of the polymer [1,2]. This allows for transport of the charge carriers in the separate materials with a low probability of recombination.

The polymer–semiconductor composites are usually prepared in the form of bilayers of the type ITO (or Au)/conducting polymer/semiconductor/metal. The ITO or Au substrates may be covered with the conducting polymer by electropolymerization or spin-casting a solution of the polymer soluble in chloroform. Semiconductor can be synthesized as a film by chemical bath deposition [3], self-assembling [4] or deposited in the form of dispersion of nanoparticles in soluble conducting

polymer [2,5–7]. The latter method is advantageous because of the increase of p–n junction interface and in effect the increase of photovoltaic efficiency. However, the semiconductor nanocrystals are not easily dispersed in conjugated polymer. A high surface energy of nanocrystals leads to their aggregation. The most efficient method of avoiding this effect is stabilization of nanocrystals by surrounding surfactant. According to the literature, the hybrid device consisting of a polymer layer and monodispersed CdS capped with thioglycerol, spin coated on the polymer film possesses a dual properties of photocurrent generation and electroluminescence [8]. However, the surfactant usually tends to isolate the semiconductor from conducting polymer phase leading to enhanced electron–hole recombination and decrease of quantum efficiency of the light energy conversion.

Another way of fabrication of semiconductor nanocluster–polymer composites is co-deposition of the two components [9]. The semiconductor nanoparticles may be also covalently linked to the monolayer assembled on Au electrode [10–12].

Preparation of the polymer–semiconductor blends is relatively easy but control of amount of two composites is problematical. In the present work we demonstrate a simple method of preparation of poly(3,4-dioctyloxythiophene)–CdS

\* Corresponding author. Tel.: +48 22 822 02 11; fax: +48 22 822 59 96.  
E-mail address: [mskomps@chem.uw.edu.pl](mailto:mskomps@chem.uw.edu.pl) (M. Skompska).

composite for photovoltaic cells. Polymer is obtained by electrodeposition, whereas CdS is formed by electrochemical/chemical synthesis. Electrochemical methods offer a wide range of control of the polymer and CdS amounts. In this work we optimize the conditions to obtain the hybrid electrode of enhanced photoactivity in comparison with that of pure CdS.

## 2. Experimental

All electrochemical measurements reported in this paper were performed by means of Autolab (EcoChemie, The Netherlands) in a three electrode cell with a platinum gauze counter electrode, Ag/AgCl, Cl<sup>-</sup> (std., aq.) reference electrode and Au working electrode. The Au substrate was polished to a mirror finish with alumina slurry and washed in an ultrasonic bath.

Procedure of synthesis and characterisation 3,4-dioctyloxythiophene (DOT) have been described elsewhere [13]. All other chemicals, LiClO<sub>4</sub> (Aldrich), Cd(ClO<sub>4</sub>)<sub>2</sub> hydrate (Aldrich), Na<sub>2</sub>S·9H<sub>2</sub>O (Aldrich) were used as received. Electrosynthesis of the polymer was performed from the solution of 10 mM DOT in acetonitrile (AN) (Aldrich, HPLC grade) containing 0.1 M LiClO<sub>4</sub> supporting electrolyte. Amount of the polymer (in mol cm<sup>-2</sup>) deposited on the electrode was estimated from the equation  $\Gamma = Q_{\text{redox}}/zF$ , where  $Q_{\text{redox}}$  is the redox charge of the polymer during cycling between 0.3 and 0.9 V in the solution of 0.1 M LiClO<sub>4</sub>/AN,  $z$  is a number of electrons involved in the redox reaction of one monomer unit ( $z=0.3$ ) and  $F$  is a Faraday constant. The estimations were not based on the polymerization charge because of some charge losses due to formation of soluble oligomers [13].

Electrodeposition of Cd was carried out from acetonitrile containing 0.1 M Cd(ClO<sub>4</sub>)<sub>2</sub> + 0.1 M LiClO<sub>4</sub>. All solutions were thoroughly deaerated by purging with dry argon for 15 min prior the experiments.

The UV–vis spectra were done using a double-beam UV/vis spectrometer (Lambda 12, Perkin-Elmer). The PDOT, CdS and PDOT/CdS for spectrophotometric measurements were deposited on ITO (indium–tin oxide)/glass electrodes (Balzers, Lichtenstein) with an area of about 2.5 cm<sup>2</sup>. The spectra were obtained for dry electrodes.

A nanoscope III (Digital Instruments, USA) was used for imaging the surfaces of the samples studied. The samples were prepared on Au substrate with an area of 0.86 cm<sup>2</sup>. AFM images in tapping mode were obtained with standard phosphorous n-doped Si cantilevers of 10 nm tip radius.

Energy dispersive X-ray spectra (EDS) were obtained by means of scanning electron microscope (LEO 435VP) equipped with a Roentec EDX analyser (model M1). Quoted elemental ratios are the mean of six values acquired by probing the film in different locations.

Photoelectrochemical experiments were carried out in the three electrode cell with a Pt counter electrode, Ag/AgCl, Cl<sup>-</sup> (std.) reference electrode and Au/CdS or Au/PDOT–CdS working electrode in deaerated aqueous solution of 0.1 M Na<sub>2</sub>S, prepared from deionised water (>18 mΩ). The working electrodes were illuminated by 450 W arc xenon lamp (Oriel). The incident power flux was passing through a 18 cm water filter. The

light intensity was measured with IL1700 Research Radiometer, (International Light, USA).

The efficiency of conversion of light energy to electric energy (power efficiency) was measured in a two electrode system, Au/CdS–PDOT/0.1 M Na<sub>2</sub>S/Pt with a variable resistance in series in the external circuit. The solution was deoxygenated with argon prior the experiments.

## 3. Results and discussion

### 3.1. Electrochemical behavior of Au/PDOT electrodes in aqueous solutions of 0.1 M LiClO<sub>4</sub> and in 0.1 M Na<sub>2</sub>S

Poly(3,4-dioctyloxythiophene) (PDOT) was deposited on Au electrode from acetonitrile solution of 10 mM monomer + 0.1 M LiClO<sub>4</sub> by cycling within the potential range from 0 to 1.34 V at the scan rate 100 mV s<sup>-1</sup>. Exemplary electropolymerization curves are presented in Fig. 1.

As visible in the inset in Fig. 1, the PDOT is electroactive not only in acetonitrile (as most of polythiophenes) but also in aqueous solution, owing to the presence of oxygen in the side groups [13]. This feature is promising in respect of application of this class of the polymers in the polymer/CdS composites.

Since the photodissolution of CdS is quenched in aqueous solution of Na<sub>2</sub>S [14], the stability of PDOT in this medium is also required. To check it and establish the most suitable potential range for further electrochemical studies, the Au/PDOT electrode was studied in deoxygenated solutions of 0.1 M Na<sub>2</sub>S in two different potential ranges: from –1.0 to –0.3 V (Fig. 2a) and from –1.0 to 0.9 V (Fig. 2b). For comparison, the similar experiments were performed in 0.1 M Na<sub>2</sub>S on a bare Au electrode. After 10 scans in each potential range the Au/PDOT electrode was transferred back into 0.1 M LiClO<sub>4</sub>/AN and cycled

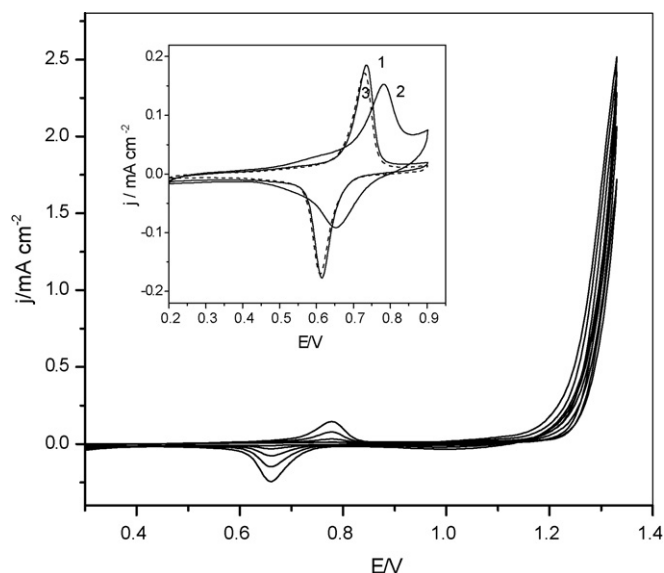


Fig. 1. Cyclic voltammograms for electropolymerization of DOT on Au electrode from the solution of 0.01 M DOT + 0.1 M LiClO<sub>4</sub>/AN. Inset: stabilized cyclic voltammograms of PDOT in the monomer-free solutions 0.1 M LiClO<sub>4</sub> in AN (curve 1) and H<sub>2</sub>O (curve 2); curve 3 corresponds to CV obtained again in AN after studies in aqueous solution.

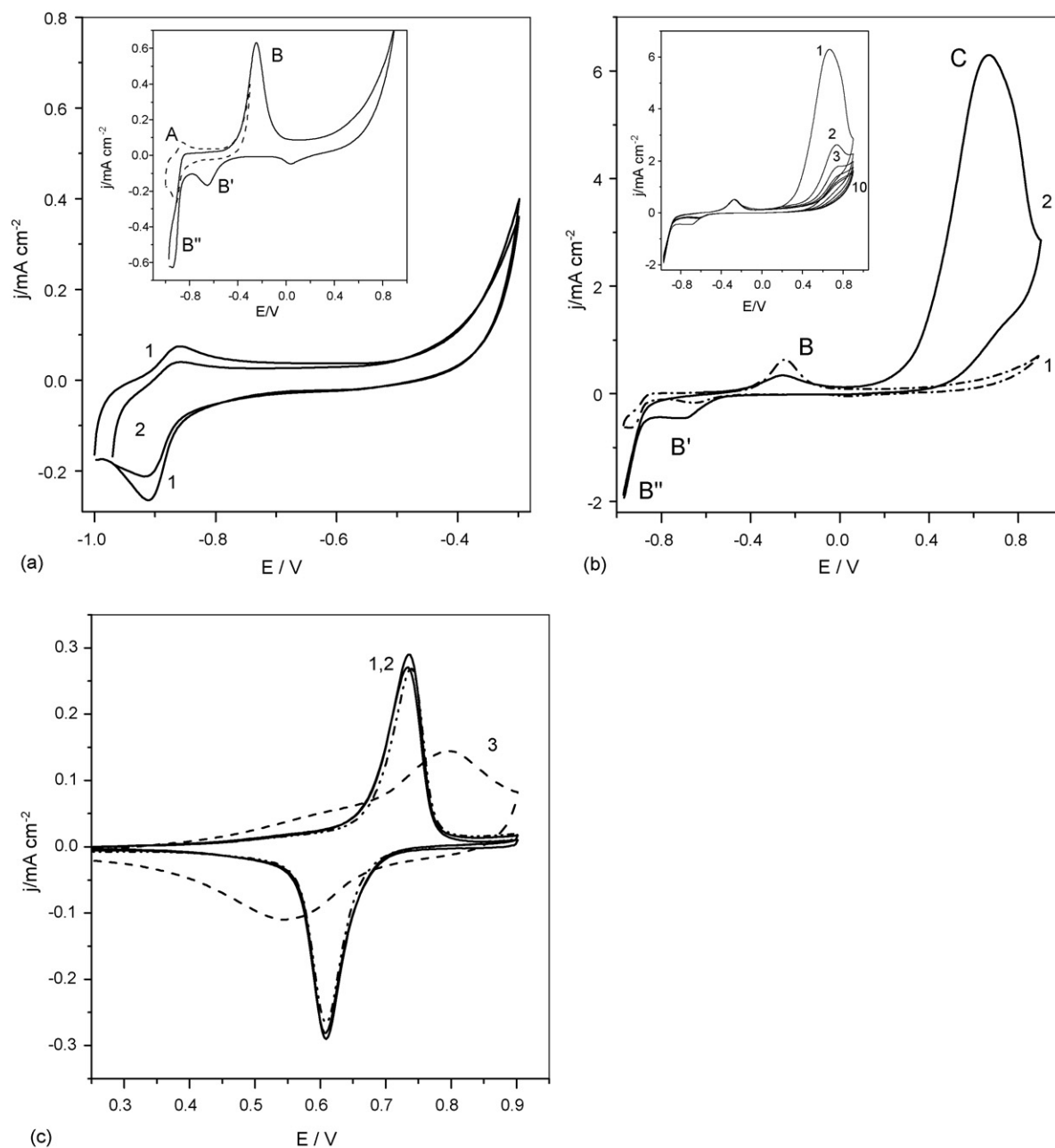
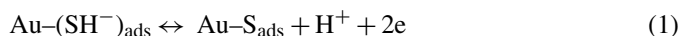


Fig. 2. (a) Cyclic voltammograms of Au (curve 1) and Au/PDOT (curve 2) electrodes in aqueous solution of 0.1 M Na<sub>2</sub>S in the potential range from -1.0 to -0.3 V. Inset: comparison of CVs at Au in two different potential ranges: from -1.0 to -0.3 V (curve A) and -1.0 to 0.9 V (curve B); (b) cyclic voltammograms of Au (curve 1) and Au/PDOT (curve 2) electrodes in 0.1 M Na<sub>2</sub>S in the potential range from -1.0 to 0.9 V; inset: subsequent CVs at Au/PDOT electrode; (c) comparison of the cyclic voltammograms in 0.1 M LiClO<sub>4</sub>/AN for the fresh Au/PDOT electrode (curve 1) and after 10 cycles in 0.1 M Na<sub>2</sub>S in the potential range from -1.0 to -0.3 V (curve 2) and in the range from -1.0 to 0.9 V (curve 3).

in the same range as before the treatment in the sulfides (Fig. 2c) to monitor the changes in the polymer electroactivity.

A pair of oxidation and reduction peaks, located respectively at -0.86 and -0.91 V, obtained during polarization of Au electrode in the potential range from -1.0 to -0.3 V (curve 1 in Fig. 2a) results from redox reaction of adsorbed SH<sup>-</sup> ions [15,16]:

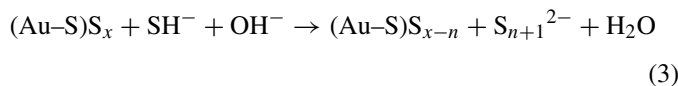


where the subscript ads refers to the adsorbed species.

Deposition of 4 nmol cm<sup>-2</sup> PDOT on Au electrode does not eliminate these peaks but only leads to some decrease of their intensity (curve 2 in Fig. 2a). This suggests that the polymer did not cover the whole substrate and SH<sup>-</sup> ions are still adsorbed on Au. As visible in Fig. 2c, the cycling of the polymer in Na<sub>2</sub>S between -1.0 and -0.3 V did not change the polymer electroactivity in acetonitrile solution (*cf.* curves 1 and 2).

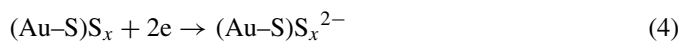
Extension of the polarization range of Au electrode to 0.9 V leads to the appearance of an anodic peak at -0.24 V (inset in Fig. 2a, peak B), related to oxidation of sulfides to sulfur and

polysulfides [15–18]:



where and  $x \geq n$ .

During the reverse scan the reduction of sulfur species occurs in two steps:



giving rise to two cathodic peaks (B' and B'') at  $-0.65$  and  $-0.94$  V.

As visible in Fig. 2b, two anodic peaks corresponding to oxidation of sulfides are observed at the Au/PDOT electrode. The first one at  $-0.24$  V (peak B) corresponds to the reaction at uncovered Au substrate, whereas the second one at  $0.67$  V (peak C) to oxidation of sulfides at the polymer/solution interface, after polymer transformation from insulating to conducting form. Enormous height of the second peak in comparison with the first one is likely due to developed surface area of the deposited polymer. Decrease of the peak intensity in the subsequent scans (see inset) suggests that the process is irreversible and the deposited sulfur blocks the polymer surface leading also to decrease of its electroactivity. This is evidenced by the change of the shape of voltammogram of Au/PDOT after transferring back into AN solution (see curve 3 in Fig. 2c).

The results presented above lead to the conclusion that the anodic potential range in the studies of Au/PDOT–CdS hybrid electrode in  $\text{Na}_2\text{S}$  should be limited to  $-0.3$  V.

### 3.2. Deposition of Cd on polymer-modified electrode

The reduction and oxidation peaks of Cd/Cd<sup>2+</sup> couple at the bare Au electrode in acetonitrile solution of 5 mM Cd(ClO<sub>4</sub>)<sub>2</sub> + 0.1 M LiClO<sub>4</sub> occur at  $-0.61$  and  $-0.23$  V, respectively (Fig. 3, curve 1). One may expect that process of Cd deposition/dissolution on the PDOT film should be hindered because of low conductivity of the polymer in the range of negative potentials, in the range between p- and n-doping [19], and dependent on the amount of the deposited polymer.

Polymerization of DOT was carried out according to the standard procedure described above. Then, the polymer-modified electrode was placed in acetonitrile solution of 5 mM Cd(ClO<sub>4</sub>)<sub>2</sub> + 0.1 M LiClO<sub>4</sub> and cycled within the potential range:  $0.1 \text{ V} \rightarrow -1.0 \text{ V} \rightarrow 0.9 \text{ V} \rightarrow 0.1 \text{ V}$  to investigate the electrochemical behavior not only in the range of cadmium deposition/dissolution but also in the zone of the polymer electroactivity. The cyclic voltammograms obtained for the electrodes covered with increasing amount of PDOT are presented in Fig. 3. The data presented in the graph and in the Table 1 indicate that the position of the reduction peak of Cd<sup>2+</sup> at PDOT-modified electrode (peak A) shifts towards more negative potentials in

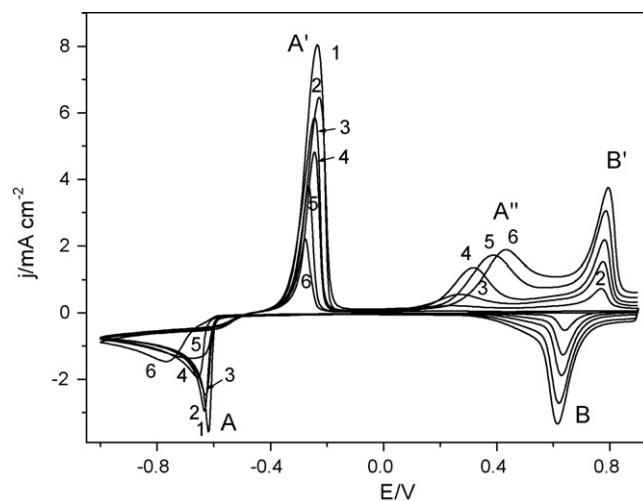


Fig. 3. Cyclic voltammograms of Au electrodes covered with different amounts PDOT, in the solution of 5 mM Cd(ClO<sub>4</sub>)<sub>2</sub> + 0.1 M LiClO<sub>4</sub>/AN in the potential range  $0.1 \text{ V} \rightarrow -1.0 \text{ V} \rightarrow 0.9 \text{ V} \rightarrow 0.1 \text{ V}$  at the scan rate  $100 \text{ mV s}^{-1}$ . The amount of the polymer deposited on Au was: (1)  $0 \text{ nmol cm}^{-2}$ , (2)  $17.5 \text{ nmol cm}^{-2}$ , (3)  $48 \text{ nmol cm}^{-2}$ , (4)  $76 \text{ nmol cm}^{-2}$ , (5)  $122 \text{ nmol cm}^{-2}$  and (6)  $161 \text{ nmol cm}^{-2}$ .

comparison to that on the bare Au electrode. However, for the polymer coverage below  $17.5 \text{ nmol cm}^{-2}$  the shift is relatively small (20 mV) and the deposition charge of cadmium is close to that obtained on the bare electrode. This is not surprising because, as it was concluded above, some parts of the substrate remained uncovered by the polymer and then Cd is mainly deposited on the bare Au.

For the higher amounts of the polymer the reduction peak shifts more strongly with complementary decrease of the deposition charge, as expected for the deposition on a low-conducting substrate. There is also a strong unbalance between reduction and reoxidation charges under the peaks A and A'. At the same time, an additional wave (A'') appears at the positive potentials at the onset of the polymer oxidation (B'). It corresponds to dissolution Cd deposited on the polymer surface—the position of peak (A'') shifts towards more positive potentials with the increase of the polymer coverage (due to increase of the polymer film resistance) and the charge under this peak is close to the “missing” charge for cadmium reoxidation (Table 1). Some charge unbalance still observed for polymer-covered electrode may be due to hindrances in oxidation of Cd deposited on the polymer surface and/or in the pores.

### 3.3. Formation of CdS and PDOT–CdS composites on the electrodes

Formation of CdS was performed according to the modified electrochemical/chemical procedure developed by Penner et al. for synthesis of semiconductor quantum dots [20]. Firstly Cd was deposited on the bare electrode (Au, Pt or ITO) or on the electrode covered with PDOT (deposited by the standard procedure) by a potential step from 0 to  $-0.74$  V versus Ag/AgCl/Cl<sup>-</sup> in the solution of 5 mM Cd(ClO<sub>4</sub>)<sub>2</sub> in AN. The amount of deposited cadmium was controlled by the reduction

Table 1

The charge densities for deposition/dissolution of Cd on the bare Au electrode and Au covered with different amounts of PDOT

$\Gamma_{\text{PDOT}}$ (nmol cm <sup>-2</sup> )	0	2.7	17.5	48	76	122	161
For polarization from 0.1 to -1.0 and back to 0.1 V							
$E_{\text{pc}}$ (V)	-0.610	-0.622	-0.632	-0.630	-0.660	-0.678	-0.766
$Q_{\text{dep(Cd)}}$ (mC cm <sup>-2</sup> ) (A)	-7.7	-7.8	-7.88	7.6	7.5	7.4	7.0
$Q_{\text{diss(Cd)}}$ (mC cm <sup>-2</sup> ) (A')	7.3	6.5	6.1	5.5	3.7	2.8	1.6
For polarization: 0 V → -1.0 V → 0.9 V → 0 V and subtraction of oxidation and reduction charges of the polymer							
$Q_{\text{dep(Cd)}}$ (mC cm <sup>-2</sup> )		7.62	7.57	7.67	7.66	7.6	7.4
$Q_{\text{diss(Cd)}}$ (mC cm <sup>-2</sup> )		7.21	7.17	7.2	6.85	6.8	6.2

charge. Then, Cd was oxidized to Cd(OH)<sub>2</sub> by immersion of the electrode in aqueous solution of 0.1 M NaOH for several minutes. Finally, Cd(OH)<sub>2</sub> was transformed into CdS by dipping the electrode for several minutes in aqueous solution of 0.1 M Na<sub>2</sub>S.

The transformation of Cd deposited on ITO or ITO/PDOT into CdS was monitored by absorption optical spectra. After each stage of transformation the ITO-modified substrate was taken out from the solution and the spectrum was done in the air within the wavelength from 1100 to 330 nm.

As visible in Fig. 4a, the spectrum after immersion of ITO/Cd in NaOH remained nearly unchanged, whereas dipping of ITO/Cd(OH)<sub>2</sub> in Na<sub>2</sub>S led to the appearance of well developed absorption peak at about 400 nm.

The spectrum of ITO covered with PDOT (Fig. 4b, curve 4), with characteristic vibronic structure, is typical of the neutral poly(3,4-dialkoxythiophenes) [13]. The data were collected in air but no increase of the absorption in the NIR range due to oxidation of the polymer was observed. After deposition of Cd on ITO/PDOT electrode and its transformation into CdS, an additional peak appeared (Fig. 4b, curve 3), similar to that visible in the spectrum of ITO/CdS. Although it is difficult to determine the absorption peak onset to estimate the value of band gap, it is evidently above 510 nm. Thus, it means that the obtained CdS particles are rather of submicron size with the bandgap close to that of the bulk CdS, i.e. 2.4 eV [21].

The EDS spectra of CdS prepared by chemical transformation of Cd, presented in Fig. 5, indicated that the CdS crystals are cadmium rich with Cd/S ratio between 2.5 and 3. The peaks at 3.13, 3.32, 3.52 and 3.72 keV with the height ratio 8:4:2:1 correspond to Cd whereas these at 2.31 and 2.46 eV (3:1) are due to the presence of S.

This Cd:S ratio is similar to that obtained from XPS spectra for CdS nanocrystals formed on HOPG by Penner et al. [22].

#### 3.4. Photoeffects of PDOT/CdS composites in aqueous solution of Na<sub>2</sub>S

The electrodes for photoelectrochemical studies were prepared on a gold substrate according to the standard procedures described above, i.e. polymerization of DOT by cyclic voltammetry, deposition of Cd by a potential step to -0.74 V and chemical transformation of Cd into CdS. Au substrate is more suitable than Pt because of better quality of ohmic contacts with semiconducting CdS film due to formation of Au-Cd alloy [23].

In order to study the influence of the amount of each component on the photoeffect, three electrodes with different amounts of PDOT and CdS were prepared, as indicated in Table 2. For comparison, the electrodes covered with only one component, PDOT or CdS were also formed.

Photoelectrochemical measurements were carried out in deoxygenated aqueous solution of 0.1 M Na<sub>2</sub>S. In the presence

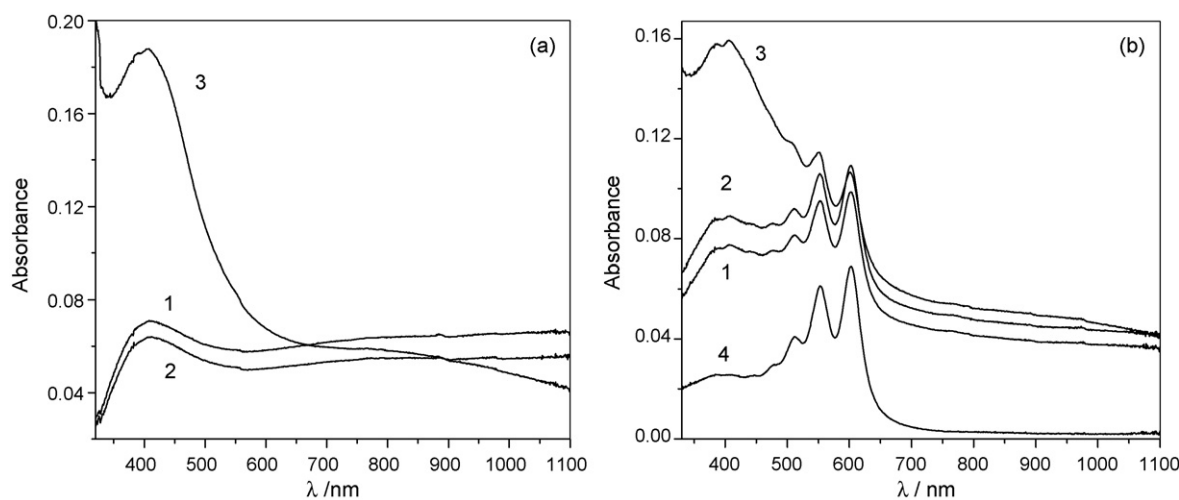


Fig. 4. Visible spectra obtained for: (a) ITO/Cd and (b) ITO/PDOT/Cd before (curves 1) and after (curves 2) treatment in 0.1 M NaOH. Curve 3 denotes the spectra after transformation of Cd(OH)<sub>2</sub> into CdS by dipping in Na<sub>2</sub>S; curve 4 in (b) corresponds to the spectrum of the neutral PDOT on ITO. All spectra were done for dry samples in air.

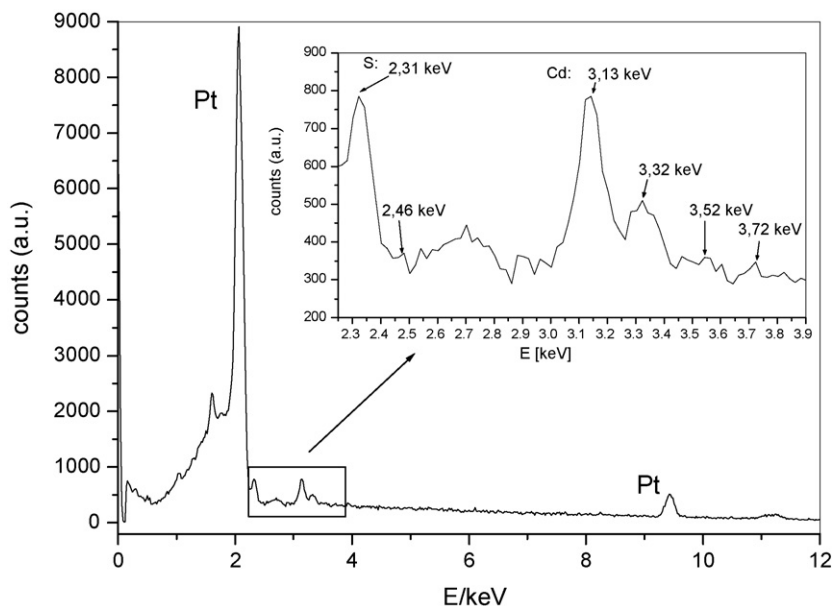


Fig. 5. EDS pattern of CdS deposited by electrochemical/chemical method on Pt.

of sulfides the holes generated in the semiconductor under illumination participate in the process of oxidation of  $S^{2-}$  to S quenching photodissolution of CdS:



However, the sulfur does not accumulate on the electrode surface but it is involved in the reaction with  $S^{2-}$  to formation of polysulfides [24]:



The electrodes were firstly cycled in dark and then under illumination. In all cases several cycles were done to stabilize the dark and the photocurrent. The experiments performed on the electrodes covered only with PDOT (PDOT4 and PDOT20, see Table 2) showed that no photocurrent was generated in polymer film cycled in aqueous solution of 0.1 M  $Na_2S$  in the potential range from  $-1.0$  to  $-0.4$  V. The differences between photocurrent and dark current for the electrodes covered with about  $4 \text{ nmol cm}^{-2}$  PDOT and two different amounts of CdS, 8 and  $20 \text{ nmol cm}^{-2}$  are presented in Fig. 6a and b, respectively. The same experiments were also carried out on the electrodes cov-

ered with the same amount of CdS but without polymer. As visible in Fig. 6a, the photoeffect obtained for the electrode covered with  $3.75 \text{ nmol cm}^{-2}$  PDOT and  $7.7 \text{ nmol cm}^{-2}$  CdS (PDOT4CdS8) is the same as that registered for the electrode decorated with the same amount of CdS but without polymer. The situation is quite different at the higher surface coverage of CdS ( $20 \text{ nmol cm}^{-2}$ ) (Fig. 6b). The photocurrent is significantly higher for the hybrid electrode PDOT4CdS20 than that for CdS without polymer (CdS20) (*cf.* curves 1 and 2 in Fig. 6b).

On the other hand, the increase of the surface coverage of the polymer to  $20 \text{ nmol cm}^{-2}$  at the same amount of CdS leads to more complicated behavior: at  $E < -0.8$  V the photoactivity of both electrodes is the same, whereas at the higher potentials the photocurrent is higher for CdS without polymer (Fig. 6c). Thus, it is evident that the ratio  $\Gamma_{\text{PDOT}}/\Gamma_{\text{CdS}}$  is a crucial parameter for photoelectrochemical properties of hybrid electrodes.

In order to explain this behavior the morphology of the electrodes covered with different amounts of CdS and PDOT was examined by means of AFM in tapping mode.

### 3.5. AFM images of Pt electrodes decorated with PDOT and CdS

The AFM images were performed both for the Au substrate covered with one of the components (PDOT or CdS) as well as with polymer–semiconductor composites, prepared as described above. The images were done for three different polymer surface coverages ( $\Gamma$ ): 3, 10 and  $17 \text{ nmol cm}^{-2}$  and two amounts of Cd: 3 and  $10 \text{ nmol cm}^{-2}$ .

According to the literature, the size and monodispersity of CdS structures obtained by *E/C* method is the same as metal crystallites deposited in the electrochemical step due to particle-by-particle conversion from metal to semiconductor [25].

As visible in Fig. 7a and b, at low coverages (between 2 and  $3 \text{ nmol cm}^{-2}$ ) the substrate is decorated with spheri-

Table 2

The surface coverages of PDOT and Cd in the electrodes prepared for the photoelectro-chemical studies

Electrode	PDOT ( $\text{nmol cm}^{-2}$ )	Cd ( $\text{nmol cm}^{-2}$ )
PDOT4CdS8	3.75	7.7
PDOT4CdS20	3.75	20
PDOT20CdS20	20	20
PDOT4	4	–
CdS8	–	7.7
PDOT20	20	–
CdS20	–	20

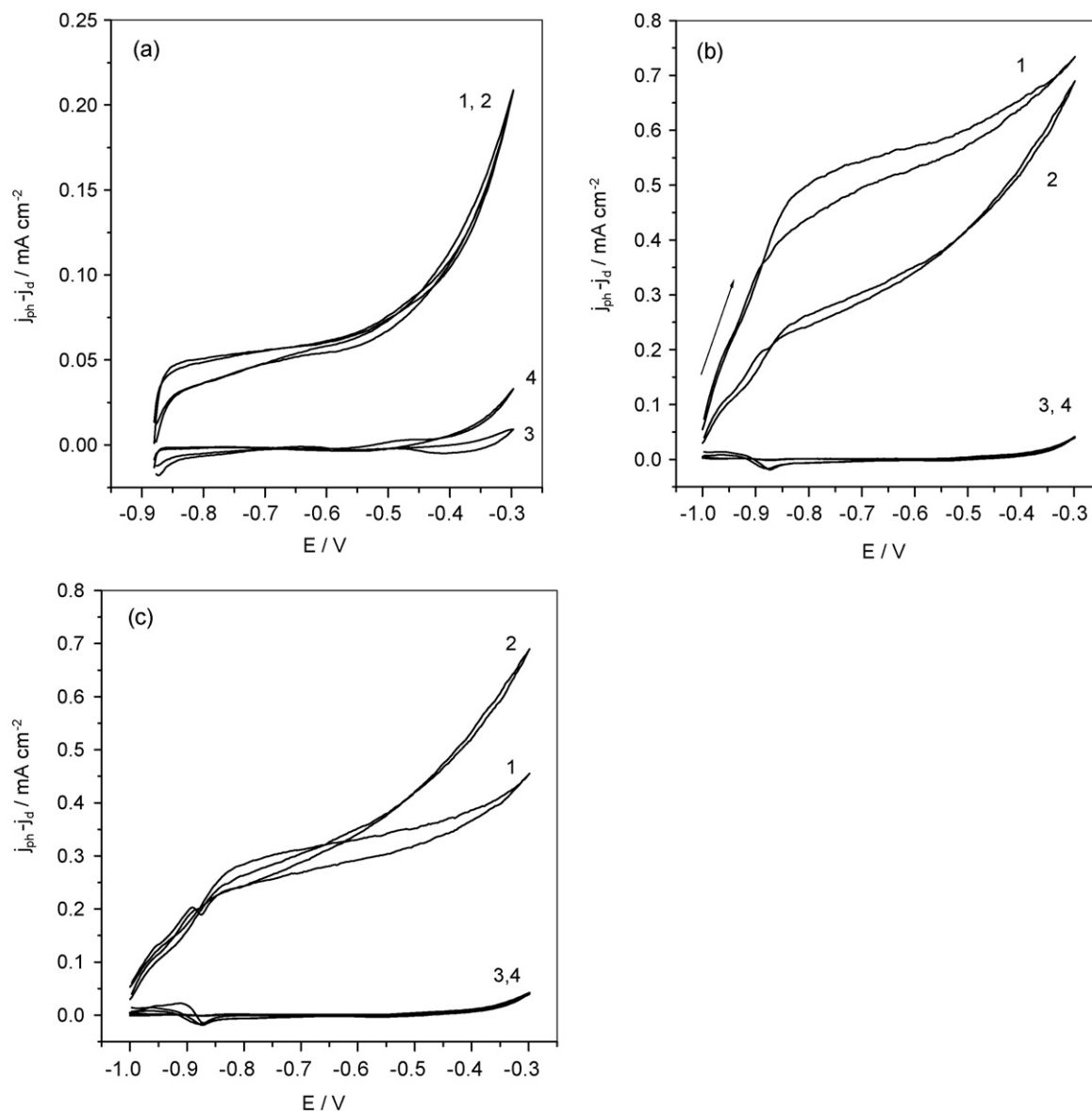


Fig. 6. Comparison of the photoeffects (difference between photocurrent and a dark current) obtained for the electrodes: (a) PDOT4CdS8 (curve 1) and CdS8 (curve 2) (see description in Table 2), (b) PDOT4CdS20 (curve 1) CdS20 (curve 2) and (c) PDOT20CdS20 (curve 1) CdS20 (curve 2) during voltammetric cycles at the scan rate  $100 \text{ mV s}^{-1}$  in the solution of  $0.1 \text{ M Na}_2\text{S}$ . Curves 3 and 4 correspond, respectively, to the voltammograms obtained at the bare Au and Au covered with corresponding amount of PDOT.

cal structures randomly distributed on the surface. The size of PDOT particles is 150–240 nm, being markedly greater than the size of CdS grains, 40–50 nm. A broad size distribution of the polymer particles results from the method of electrodeposition. During each voltammetric cycle the new “nucleation” centers are formed, whereas the old ones are growing up. A general image of the substrate covered with CdS obtained at low deposition charge is similar to that presented by Gorer et al. [25] but a distribution of the particles is less uniform and their size is about 10 times larger. This is due to different electrodeposition conditions i.e. different substrate, non-aqueous solvent, longer potential pulses and smaller overpotential applied. However, the goal of our experiments was also different and deposition of nano-sized CdS particles was not our intention.

As visible in Fig. 7c, at the higher PDOT coverages the polymer grains tend to coalesce forming the islands of dense, three-dimensional aggregates of independent particles, which finally start to cover the whole substrate. However, even at  $\Gamma = 17 \text{ nmol cm}^{-2}$  some parts of the substrate remained still uncovered (Fig. 7e), which is consistent with the conclusions derived from the cyclic voltammograms obtained for deposition of Cd and oxidation of sulfides on the PDOT-modified electrodes.

At the CdS coverage of  $10 \text{ nmol cm}^{-2}$ , the surface is covered with a uniform “layer” of independent particles and the size distribution of CdS grains is still relatively narrow (60–80 nm) (Fig. 7d). Thus, it seems that deposition of Cd occurs via instantaneous nucleation, as has been suggested by Gorer et al. [25]. According to the literature, the nearest neighbor distance of

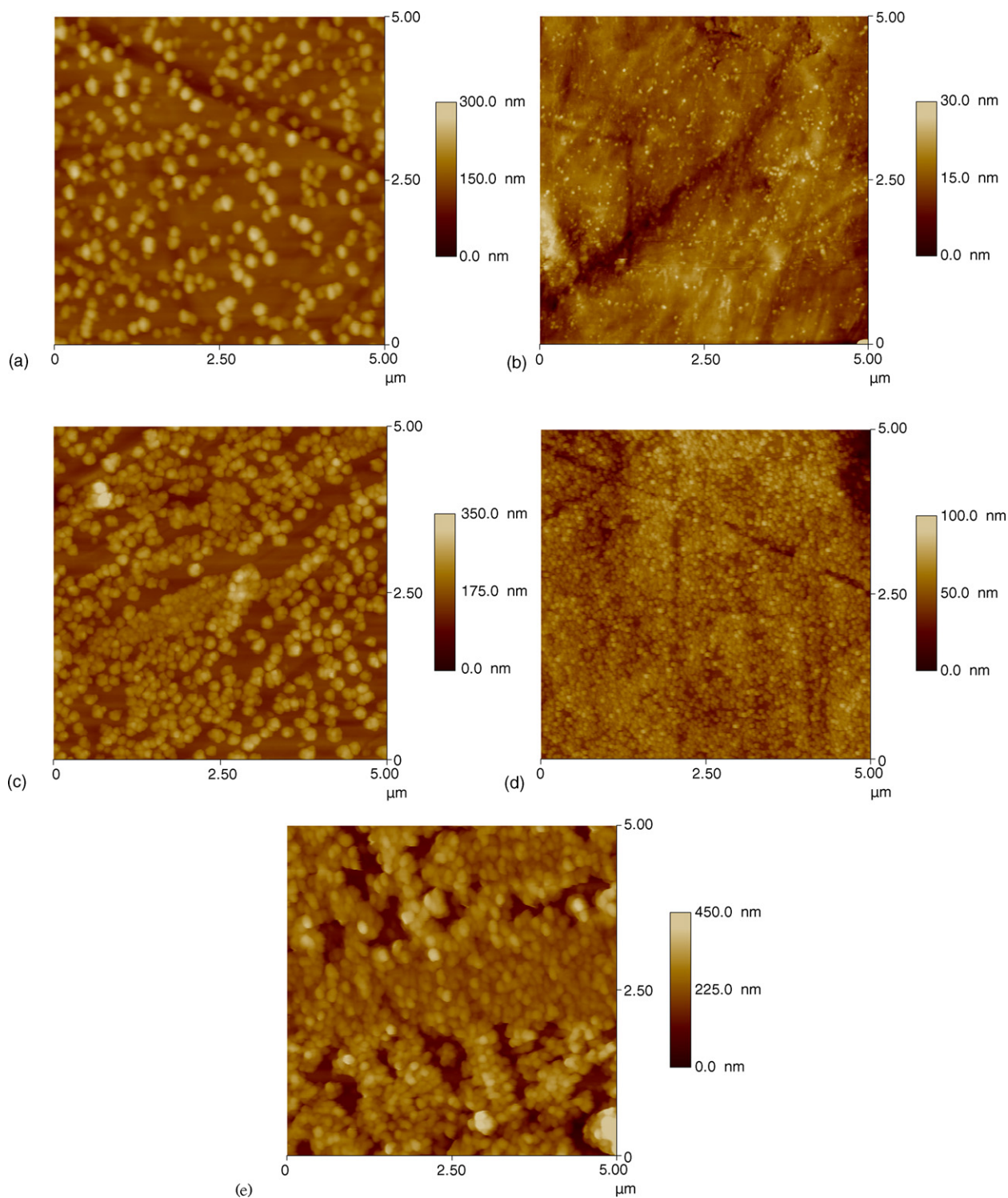


Fig. 7. AFM images for Au substrate covered with: (a)  $2.8 \text{ nmol cm}^{-2}$  of PDOT, (b)  $2 \text{ nmol cm}^{-2}$  of CdS, (c)  $10 \text{ nmol cm}^{-2}$  of PDOT, (d)  $10 \text{ nmol cm}^{-2}$  of CdS and (e)  $17 \text{ nmol cm}^{-2}$  of PDOT.

$0.289 \text{ nm}$  for hexagonal packed layer Cd gives a coverage of  $2.16 \text{ nmol cm}^{-2}$ . The studies of underpotential Cd deposition by means of EQCM on the polycrystalline Au from aqueous solution of  $\text{HClO}_4$  gave even lower value of  $1.4 \text{ nmol cm}^{-2}$  [26]. Thus, at  $\Gamma = 10 \text{ nmol cm}^{-2}$  the surface should be covered with amount corresponding to about five monolayers of Cd.

Now, having a picture of the PDOT and CdS deposits, one can explain the differences in the photoeffects of hybrid electrodes at various polymer and cadmium coverages. It should be stressed however, that the images presented in Fig. 7 do not reflect exactly the distribution of the particles on the whole substrate of an area  $0.86 \text{ cm}^2$ —some parts were covered by more and other by less densely distributed particles.

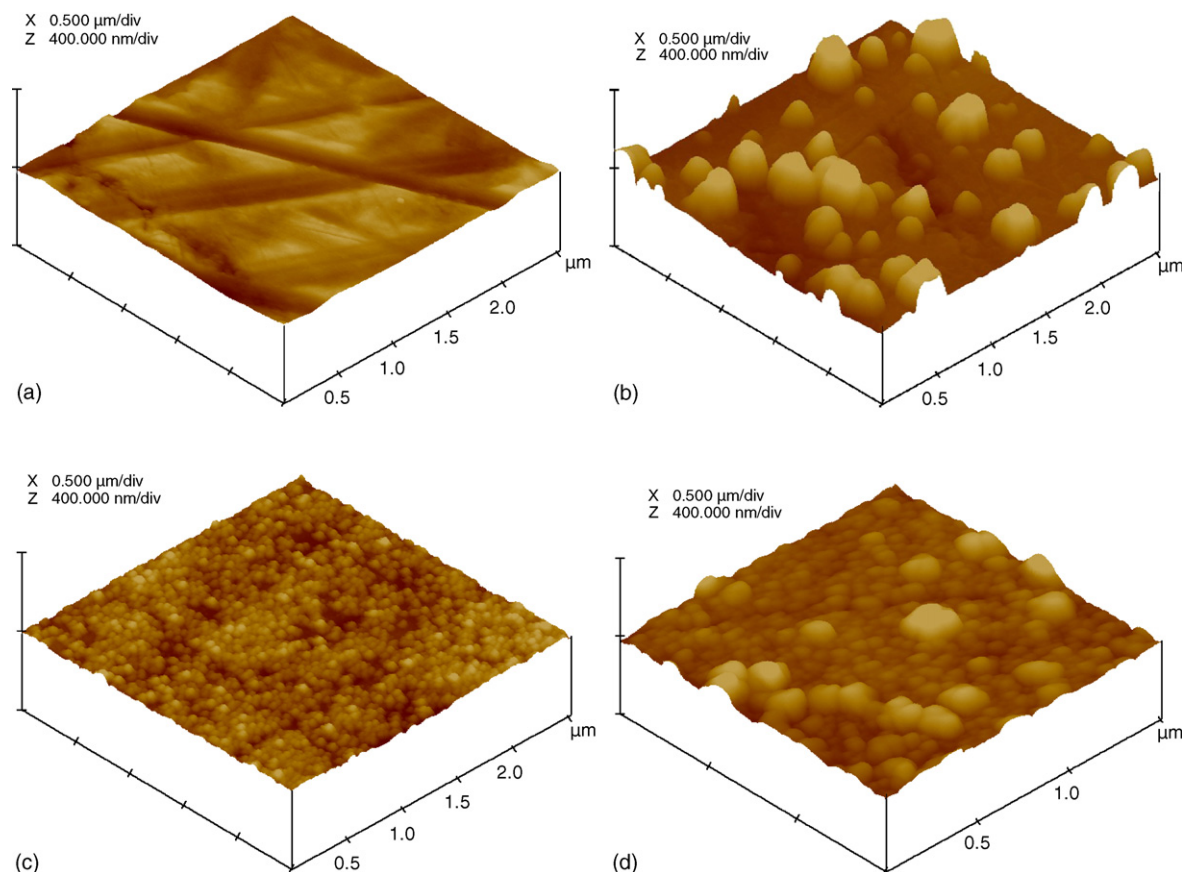


Fig. 8. Surface three-dimensional topography of the bare Au substrate (a); PDOT ( $4 \text{ nmol cm}^{-2}$ ) (b); CdS ( $10 \text{ nmol cm}^{-2}$ ) (c); PDOT–CdS hybrid electrode ( $4 \text{ nmol cm}^{-2}$  PDOT and  $10 \text{ nmol cm}^{-2}$  Cd) (d).

Nevertheless, one can expect that at low amounts of both components, the particles of PDOT and CdS probably exist on the substrate independently and the polymer does not influence the photoeffect of CdS. At the higher amount of CdS (PDOT4CdS20) both type of the species (polymer and semiconductor) are likely located in close proximity to one another. Since the polymer and CdS have different electron affinity the charge carriers generated in the semiconductor under illumination may be easily separated – the electrons are transported to the metal substrate, whereas the holes are transferred to the polymer and then may be consumed in the reaction with  $\text{S}^{2-}$  from the solution. Accommodation of the holes by the polymer results in significant inhibition of the electron–hole recombination in the semiconductor and in the increase of the photoeffect in comparison to that for CdS without polymer (CdS20).

The arrangements of PDOT, CdS and both components in the hybrid electrode are clearly illustrated in the three-dimensional images presented in Fig. 8.

At the higher polymer coverages (PDOT20CdS20), the area of uncovered Au is limited and Cd deposition takes place also on the surface of PDOT. However, the relatively high resistivity of the polymer in the range of negative potentials results in slowing down the transport of the electrons from CdS to the metal contact and therefore, the photocurrent is lower than that observed for CdS without polymer.

### 3.6. Photovoltaic properties of the electrochemical cell based on CdS–PDOT hybrid electrode

To determine the conversion efficiency of light energy to electrical energy (power efficiency),  $\eta$ , the photoelectrochemical cell was connected in series with a variable load resistance. The current–potential curve was obtained for resistances ranging from  $20 \text{ M}\Omega$  to  $100 \Omega$ . The measurements were performed in dark and under illumination and the results were used to determine the power characteristic of the cell.

The power efficiency, in percent, was calculated using the equation:

$$\eta (\%) = \frac{P_{\max}}{P_{\text{in}}} \times 100 \quad (9)$$

where  $P_{\max}$  is a maximum power of the cell, whereas  $P_{\text{in}}$  denotes the power input (in our case  $200 \text{ mW cm}^{-2}$ ). The quality of the cell was also determined by a fill factor, FF, defined as

$$\text{FF} = \frac{I_{\max} U_{\max}}{I_{\text{sc}} U_{\text{oc}}} \quad (10)$$

where  $I_{\max}$  and  $U_{\max}$  are the photocurrent and photopotential corresponding to the maximum power,  $I_{\text{sc}}$  is a short-circuit current, i.e. maximum photocurrent observed when the resistance of the circuit between the cell terminals is zero (at zero photopotential) whereas  $U_{\text{oc}}$  is the open-circuit potential corresponding

Table 3  
Photovoltaic properties of hybrid CdS–PDOT/0.1 M Na<sub>2</sub>S electrochemical cell

$I_{sc}$ (mA cm <sup>-2</sup> )	0.58
$U_{oc}$ (V)	0.52
FF	0.51
$P_{max(out)}$ (mW)	0.03
$\eta$ (%)	0.1

to zero photocurrent (when the external resistance is very large ( $R \rightarrow \infty$ )).

The photovoltaic properties of the cell based on CdS–PDOT hybrid electrode composed of 4 nmol cm<sup>-2</sup> PDOT and 20 nmol cm<sup>-2</sup> CdS are listed in Table 3.

The obtained photovoltaic parameters are lower than those reported recently by Kang and Kim [27] ( $\eta = 0.6\%$ , FF = 0.496,  $V_{oc} = 0.858$  V and  $I_{sc} = 1.39$  mA cm<sup>-2</sup>) for the system composed of vertically aligned CdS nanorods in poly[2-methoxy-5-(2'-ethylhexoxy)-1,4-phenylene-vinylene (MEH-PPV). However, the electron transport in the aligned nanorods is remarkably faster than that in the spherical structures obtained by electrodeposition. According to the literature [28,29], the enhancement of solar energy conversion efficiency may be achieved by thermal treatment of the hybrid system. This effect was attributed to reorganization of the CdS nanocrystals/polymer interface leading to an increase of exciton dissociation efficiency [29]. This raises expectation that annealing should also improve the properties of the CdS–PDOT composite and our work will be continue in this direction.

#### 4. Conclusions

Au/poly(3,4-dioctyloxythiophene)–CdS hybrid electrodes have been prepared by means of four-step electrochemical/chemical method. Au was firstly decorated with the polymer by cyclic voltammetry and then, CdS was formed by potentiostatic deposition of Cd followed by its chemical transformation into Cd(OH)<sub>2</sub> in NaOH and finally to CdS by immersion in Na<sub>2</sub>S. The CdS crystals obtained by this procedure are cadmium rich with Cd/S ratio from 2.5 to 3.

CdS and PDOT are deposited in the form of hemispherical structures dispersed on the substrate. Their size and density may be easily controlled by the electrodeposition charge.

The amount of both components and the CdS:PDOT ratio are crucial for photoelectroactivity of the hybrid electrodes in aqueous solution of 0.1 M Na<sub>2</sub>S. In the most suitable conditions the polymer structures adjacent to the semiconductor particles play role of acceptors of the holes generated under illumination, whereas the semiconductor transports the electrons to the metal substrate. The charge separation results in significant inhibition of the electron–hole recombination and enhancement of the photoeffect. The photovoltaic device based on the spherical CdS structures and electrochemically synthesized PDOT provided

energy conversion efficiency of 0.1%, open circuit voltage of 0.52 V, short circuit photocurrent density of 0.58 mA cm<sup>-2</sup> and fill factor of 0.51. The improvement of these parameters can be likely achieved by annealing of the hybrid electrode.

#### Acknowledgements

Support for this work by the Polish Ministry of Education and Science under grants 3T08A04128 and N20409131/2142 is gratefully acknowledged.

#### References

- [1] N.C. Greenham, P. Xiaogang, A.P. Alivisatos, *Phys. Rev. B* 54 (1996) 17628.
- [2] D.S. Gringer, N.C. Greenham, *Phys. Rev. B* 59 (1999) 10622.
- [3] P. Chartier, H. Nguyen Cong, C. Sene, *Solar Energy Mater.* 52 (1998) 413.
- [4] T. Cassagneau, T.E. Mallouk, J.H. Fendler, *J. Am. Chem. Soc.* 120 (1998) 7848.
- [5] W.U. Huynh, J.J. Dittmer, A.P. Alivisatos, *Science* 295 (2002) 2425.
- [6] E. Arici, H. Hoppe, F. Schäffler, D. Meissner, M.A. Malik, N.S. Sariciftci, *Thin Solid Films* 451/452 (2004) 612.
- [7] W.U. Huynh, J.J. Dittmer, W.C. Libby, G.L. Whiting, A.P. Alivisatos, *Adv. Funct. Mater.* 13 (2003) 73.
- [8] K.S. Narayan, A.G. Manoy, J. Nanda, D.D. Sarma, *Appl. Phys. Lett.* 74 (1999) 871.
- [9] S. Pethkar, R.C. Patil, J.A. Kher, K. Vijayamohan, *Thin Solid Films* 349 (1999) 105.
- [10] T. Nakanishi, B. Ohtani, K. Uosaki, *J. Phys. Chem. B* 102 (1998) 1571.
- [11] L. Sheeney-Haj-Ichia, J. Wasserman, I. Willner, *Adv. Mater.* 14 (2002) 1323.
- [12] E. Granot, F. Patolsky, I. Willner, *J. Phys. Chem. B* 108 (2004) 5875.
- [13] A. Szkurlat, B. Palys, J. Mieczkowski, M. Skompska, *Electrochim. Acta* 48 (2003) 3665.
- [14] A.B. Ellis, S.W. Kaiser, J.M. Bolts, M.S. Wrighton, *J. Am. Chem. Soc.* 99 (1977) 2839.
- [15] R.O. Lezna, N.R. De Tacconi, A.J. Arvia, *J. Electroanal. Chem.* 283 (1990) 319.
- [16] X. Gao, Y. Zhang, M.J. Weaver, *Langmuir* 8 (1992) 668.
- [17] A.N. Buckley, I.C. Hamilton, R. Woods, *J. Electroanal. Chem.* 216 (1987) 213.
- [18] N. Myung, S. Ham, B. Choi, N.R. de Tacconi, K. Rajeshwar, *J. Electroanal. Chem.* 574 (2005) 367.
- [19] M. Skompska, J. Mieczkowski, R. Holze, J. Heinze, *J. Electroanal. Chem.* 57 (2005) 9.
- [20] M.A. Anderson, S. Gorer, R.M. Penner, *J. Phys. Chem. B* 101 (1997) 5895.
- [21] A. Henglein, *Chem. Rev.* 89 (1989) 1861.
- [22] S. Gorer, J.A. Ganske, J.C. Hemminger, R.M. Penner, *J. Am. Chem. Soc.* 120 (1998) 9584.
- [23] J.J. Kelly, J.M.G. Rikken, J.W.M. Jacobs, A. Valster, *J. Vac. Sci. Technol. B* 6 (1988) 48.
- [24] B. Miller, A. Heller, *Nature* 262 (1976) 680.
- [25] S. Gorer, G.S. Hsiao, M.G. Anderson, R.M. Stiger, J. Lee, R.M. Penner, *Electrochim. Acta* 43 (1998) 2799.
- [26] M.R. Deakin, O. Melroy, *J. Electroanal. Chem.* 239 (1988) 321.
- [27] Y. Kang, D. Kim, *Solar Energy Mater. Solar Cells* 90 (2006) 166.
- [28] W.J.E. Beek, M.M. Wienk, R.A.J. Janssen, *Adv. Funct. Mater.* 16 (2006) 1112.
- [29] L. Wang, Y.S. Liu, X. Jiang, D.H. Quin, Y. Cao, *J. Phys. Chem. C* 111 (2007) 9538.